HHS Public Access

Author manuscript

Plant J. Author manuscript; available in PMC 2016 September 01.

Published in final edited form as:

Plant J. 2016 March ; 85(5): 594–606. doi:10.1111/tpj.13093.

The PPR-SMR protein PPR53 enhances the stability and translation of specific chloroplast RNAs in maize

Reimo Zoschke[1,2], **Kenneth P. Watkins**[1], **Rafael G. Miranda**[1], and **Alice Barkan**[1,*]

Reimo Zoschke: reimo.zoschke@gmx.de; Kenneth P. Watkins: watkins@uoregon.edu; Rafael G. Miranda: rafaelm@uoregon.edu

[1]Institute of Molecular Biology, University of Oregon, Eugene, OR 97403

Summary

Pentatricopeptide repeat (PPR) proteins are helical repeat proteins that bind RNA and influence gene expression in mitochondria and chloroplasts. Several PPR proteins in plants harbor a carboxy-terminal Small-MutS-Related (SMR) domain, but functions of the SMR appendage are unknown. To address this issue, we studied a maize PPR-SMR protein denoted PPR53 (GRMZM2G438524), which is orthologous to the Arabidopsis protein SOT1 (AT5G46580). Null *ppr53* alleles condition a chlorotic, seedling lethal phenotype and a reduction in plastid ribosome content. Plastome-wide transcriptome and translatome analyses revealed strong defects in the expression of the *ndhA* and *rrn23* genes, which were superimposed on secondary effects resulting from a decrease in plastid ribosome content. Transcripts with processed 5′-ends mapping approximately 70-nt upstream of *rrn23* and *ndhA* are absent in *ppr53* mutants, and the translational efficiency of the residual *ndhA* mRNAs is reduced. Recombinant PPR53 binds with high affinity and specificity to the 5′ proximal region of the PPR53-dependent 23S rRNA, suggesting that PPR53 protects this RNA via a barrier mechanism similar to that described for several PPR proteins lacking SMR motifs. However, recombinant PPR53 did not bind with high affinity to the *ndhA* 5′ UTR, suggesting that PPR53's RNA stabilization and translation enhancing effects at the *ndhA* locus involve the participation of other factors.

Keywords

pentatricopeptide repeat; SMR domain; chloroplast; plastid; RNA processing; translational activator; *Zea mays*

Introduction

Gene expression systems in mitochondria and chloroplasts are derived from those in their bacterial progenitors, but they have acquired many new features during their coevolution with the eucaryotic host (reviewed in Barkan, 2011a; Hammani and Giege, 2014). For example, organellar RNAs in plants are modified by RNA editing, RNA splicing, and by exo- and endonucleolytic processing events that are either unusual or absent in bacteria. Many of these events are mediated by nucleus-encoded RNA binding proteins in the alpha

*Author to whom correspondence should be addressed: abarkan@uoregon.edu, Tel: 541-346-5145, FAX: 541-346-5891.

[2]Current address: Max Planck Institute of Molecular Plant Physiology, 14476 Potsdam-Golm, Germany.

solenoid superfamily, which are characterized by tracts of tandem helical repeats (Hammani *et al.*, 2014). The pentatricopeptide repeat (PPR) protein family (Small and Peeters, 2000) is the canonical example of this phenomenon. PPR proteins are found in all eucaryotes and function almost exclusively in organellar gene expression (reviewed in Barkan and Small, 2014). They influence a wide range of molecular processes, including RNA editing, RNA stabilization, group II intron splicing, RNA cleavage and translation. Many PPR proteins bind specific RNA sequences and do so, at least in part, via a modular 1 repeat-1 nucleotide binding mode in which several amino acids in each repeat specify the bound nucleotide via a predictable "code" (Barkan *et al.*, 2012; Takenaka *et al.*, 2013; Yagi *et al.*, 2013a).

PPR proteins fall into several subfamilies based on the nature of their repeats and on the presence or absence of additional functional domains (Lurin *et al.*, 2004). Roughly half of the PPR proteins in plants consist of PPR tracts and little else; functions ascribed to these "pure" PPR proteins include enhancement of group II intron splicing, RNA stabilization, definition of processed RNA termini, translational activation and repression, and the promotion of site-specific RNA cleavages (reviewed in Barkan and Small, 2014). Several of these functions have been shown to result from passive steric effects caused by the high affinity binding of an RNA segment along the extended surface of a long PPR tract. For example, this type of activity defines and stabilizes specific processed RNA termini (Pfalz *et al.*, 2009; Ruwe and Schmitz-Linneweber, 2012; Zhelyazkova *et al.*, 2012; Fujii *et al.*, 2013; Haili *et al.*, 2013), and guides RNA folding in a manner that increases translational efficiency (Prikryl *et al.*, 2011; Zoschke *et al.*, 2013b). Another large subset of PPR proteins in plants harbor variant repeat tracts followed by characteristic carboxy-terminal domains that are required to direct sites of RNA editing in mitochondria and chloroplasts (reviewed in Yagi *et al.*, 2013b).

A small PPR subfamily is characterized by a PPR tract followed by a carboxy-terminal Small MutS Related (SMR) domain (reviewed in Liu *et al.*, 2013). These "PPR-SMR" proteins comprise approximately eight orthologous groups in angiosperms. The PPR-SMR subfamily has attracted considerable attention due to the physiological functions ascribed to several of its members. For example, GUN1 influences the transcription of nuclear genes in response to certain types of plastid dysfunction (Koussevitzky *et al.*, 2007), albeit through unknown mechanisms. PTAC2 associates with the plastid-encoded RNA polymerase (PEP) and is required for its activity (Pfalz *et al.*, 2006), but the basis for this effect is unknown. Orthologous proteins denoted SVR7 in *Arabidopsis thaliana* and ATP4 in *Zea mays* have overlapping but distinct effects on chloroplast gene expression. SVR7 was recovered in a genetic screen for suppressors of a leaf variegation phenotype (Liu *et al.*, 2010). Loss of SVR7 function causes mild defects in plant growth, chloroplast rRNA processing, and the accumulation of the chloroplast ATP synthase (Liu *et al.*, 2010; Zoschke *et al.*, 2013a). By contrast, ATP4 is required for the translation of the *atpB* open reading frame (ORF) and for the accumulation of specific processed transcript isoforms from the *atpF*, *psaJ*, and *rpl14* loci (Zoschke *et al.*, 2012; Zoschke *et al.*, 2013b). It has been shown that ATP4 associates *in vivo* with the 5′UTR of the *atpB* mRNA (Zoschke *et al.*, 2012), but beyond that, mechanisms underlying these effects are unknown.

It seems likely that the SMR domain expands the functional repertoire of the PPR tract, but there is little information about the nature of its contribution. SMR domains in other contexts have been shown to harbor DNA or RNA endonuclease activity and to bind branched DNA structures (reviewed in Fukui and Kuramitsu, 2011). In addition, SMR domains are structurally similar to several known DNA and RNA binding domains (reviewed in Fukui and Kuramitsu, 2011). These findings provide a foundation for hypotheses concerning the functions of the SMR domain in PPR-SMR proteins, but alternative possibilities are also plausible.

To elucidate the functions of the SMR domain in PPR-SMR proteins, we studied the molecular functions of the maize PPR-SMR protein encoded by gene GRMZM2G438524. This protein, denoted here as PPR53, is orthologous to Arabidopsis SOT1 (AT5G46580). Our results indicate that PPR53 harbors several molecular functions that have been ascribed also to PPR proteins lacking an SMR domain: it can serve as a site-specific blockade to 5′→3′ RNA decay and it can stimulate the translation of a specific mRNA. We detected two sites of PPR53 action, one in a precursor to the 23S rRNA and the other in the *ndhA* 5′UTR. PPR53 is required for the accumulation of 23S rRNA precursors with a 5′ end mapping 73 nucleotides upstream of mature 23S rRNA. PPR53 binds directly to this site, as shown by *in vitro* RNA binding assays and by the fact that its sequence matches that predicted for the PPR53 binding site based on the PPR code. PPR53 also stabilizes RNAs with a processed 5′-end 66 nucleotides upstream of *ndhA* and increases the translational efficiency of the *ndhA* open reading frame (ORF). However, PPR53 did not bind with high affinity to the *ndhA* 5′UTR *in vitro*, and the sequence of the *ndhA* 5′UTR shows little similarity to PPR53's predicted binding site. These features are reminiscent of an activity described for the PPR-SMR protein ATP4, which is required to support the action of the pure PPR protein PPR10 when it stabilizes the 3′-terminus of *psaJ* mRNA (Zoschke *et al.*, 2012). As such, we suggest that PPR53 promotes the binding of a different, as yet unidentified protein to the *ndhA* 5′UTR, which acts directly to block a 5′→3′ exoribonuclease and to stimulate *ndhA* translation.

Results

Disruption of *ppr53* causes a mild global loss of plastid-encoded proteins and a severe loss of the plastid NDH complex

PPR53 and its orthologs consist of a predicted chloroplast targeting sequence followed by a conserved segment lacking known functional motifs, eleven PPR motifs, and an SMR domain (Figure 1a and Figure S1 in Supporting Information). Two insertions in *ppr53* were identified during the systematic sequencing of *Mu* transposon insertions in mutants in the Photosynthetic Mutant Library (Belcher *et al.*, 2015), each of which cosegregated with a recessive mutation conditioning a range of chlorotic phenotypes (Figure 1a). Complementation crosses between plants that were heterozygous for each allele produced heteroallelic progeny with chlorotic phenotypes (Figure 1a), confirming that the mutant phenotypes result from disruption of the *ppr53* locus. Both alleles are likely to be null alleles based on the positions of the insertions in the gene and the fact that mRNA derived from sequences flanking the insertions was below the limit of detection by RT-PCR (Figure 1b).

The basis for the variability in phenotype is unknown, but might be due to the segregation of polymorphic modifier loci, to unusual sensitivity to local environmental conditions, or to stochastic effects early in development.

Given the functions established for characterized PPR proteins and the fact that PPR53 is an abundant component of the chloroplast nucleoid (Majeran *et al.*, 2012), it seemed likely that the chlorotic phenotypes of *ppr53* mutants result from a defect in chloroplast gene expression. As a first step toward characterizing chloroplast gene expression in *ppr53* mutants, immunoblots of seedling leaf extracts were probed to detect core subunits of each photosynthetic complex harboring plastid-encoded proteins: photosystem I (PSI), photosystem II (PSII), the cytochrome b_6f complex, the ATP synthase, the NADH dehydrogenase-like complex (NDH), and Rubisco (Figure 2). The failure to synthesize or assemble any core subunit of these complexes is generally accompanied by a reduction in the levels of closely-associated subunits. Mutant *ppr53* individuals exhibiting a range of chlorotic phenotypes were compared with a mutant lacking ATP4, which is the most closely related paralog of PPR53 (Liu *et al.*, 2013) (see Figure S1). As shown previously (Zoschke *et al.*, 2012), *atp4* mutants have a strong and rather specific loss of ATP synthase subunits (AtpB and AtpF). By contrast, *ppr53* mutants displayed a severe deficiency for NdhH, a subunit of the NDH complex. This strong NDH defect is superimposed on a moderate loss of components of the ATP synthase, PSII, PSI, cytochrome b_6f, and Rubisco. The latter deficiencies ranged from roughly 25%–50% of normal levels, with the severity of the protein defects correlating with that of the chlorotic phenotype. Taken together, these results suggested that PPR53 plays a critical role in the expression of at least one subunit of the NDH complex, and that it also boosts overall plastid gene expression.

Genome-wide analyses of the plastid transcriptome and translatome in *ppr53* mutants revealed defects in *ndhA* and *rrn23* expression

To further define the effects of PPR53 on plastid gene expression, the expression of all chloroplast genes in *ppr53* mutants was analyzed with a ribosome profiling method that provides a genome-wide, quantitative read-out of mRNA abundance and ribosome occupancy (Zoschke *et al.*, 2013b). The method employs high-resolution microarrays to quantify “ribosome footprints” (mRNA segments that are protected by ribosomes from nuclease attack) derived from all chloroplast open reading frames, at a resolution of ~30 nucleotides. The ratios of ribosome footprint signals in the wild-type relative to the *ppr53* mutant are plotted according to position on the chloroplast genome in Figure 3b. A prominent peak was detected that mapped to *ndhA*, indicating that *ppr53* mutants have a strong defect in *ndhA* expression. A modest decrease in expression of the adjacent downstream gene *ndhI* is apparent in a high-resolution view of the data (Figure 3e). The abundance of ribosome footprints on other genes encoding NDH subunits was similar to that in the wild-type. The loss of NdhH protein in *ppr53* mutants can be explained by the defect in *ndhA* expression, as NdhA and NdhH belong to NDH subcomplex A, whose members fail to accumulate when one subunit is not synthesized or assembled (reviewed in Ifuku *et al.*, 2011).

Hybridization of seedling leaf RNA from wild-type and mutant seedlings to the same microarray format (Figure 3c) showed that *ndhA* RNA accumulates to near normal levels in *ppr53* mutants, indicating that the defect in *ndhA* expression is largely due to decreased translational efficiency (Figure 3d). In addition, the transcriptome data revealed a substantial decrease in the abundance of rRNAs of the large ribosomal subunit (23S, 4.5S and 5S). Several other minor differences between the mutant and wild-type transcriptomes were observed (e.g. a slight loss of *psbA* RNA, 16S rRNA and several tRNAs), but similar changes have been observed in other mutants with modest chloroplast ribosome deficiencies (Williams-Carrier *et al.*, 2014) suggesting that these are secondary effects of the reduced ribosome content in *ppr53* mutant chloroplasts (see below).

PPR53 is required for the accumulation of RNAs with processed 5′-ends upstream of *ndhA* and *rrn23*

Several PPR proteins that activate the translation of specific chloroplast RNAs also stabilize processed mRNAs from the same gene (Barkan *et al.*, 1994; Pfalz *et al.*, 2009; Cai *et al.*, 2011; Zoschke *et al.*, 2013b). To determine whether PPR53 has dual effects of this nature, transcripts from the *ndhA* transcription unit were analyzed by RNA gel blot hybridization (Figure 4). The *ndhA* gene includes a group II intron and is embedded in a polycistronic transcription unit that gives rise to a complex population of processed RNAs (see, for example, del Campo *et al.*, 2000). The transcripts from the *ndhA* transcription unit have not been comprehensively mapped in any species. We inferred the positions of some transcripts based on their size, the probes to which they hybridized, and the positions of processed termini that have been mapped in barley and/or maize (Zhelyazkova *et al.*, 2012) (Figure 4a). However, the large size and comigration of many of the transcripts precluded their firm placement on the map.

Despite this limitation, the results show that several *ndhA* transcript isoforms were missing in *ppr53* mutants but accumulate normally in other non-photosynthetic mutants that were analyzed as controls (Figure 4a). This is not due to the failure to splice the *ndhA* intron because the excised intron accumulated to normal levels in *ppr53* mutants (see transcript 3 in Figure 4a), and both spliced and unspliced transcript isoforms were missing (see for example transcripts 4, 5, and 6 in Figure 4a). Instead, the results suggested that PPR53 is required for the accumulation of transcripts with a 5′ end mapping a short distance upstream of the *ndhA* gene (see transcripts 4 through 8 in Figure 4a). A processed 5′ end mapping 66 nucleotides upstream of *ndhA* has been mapped in barley and maize (Zhelyazkova *et al.*, 2012), and the RNA gel blot data suggested that transcripts with this end require PPR53 for their accumulation. To test this possibility, we used a poisoned-primer extension assay, which compiled all 5′-processed *ndhA* transcript isoforms into one band, and all isoforms with distal 5′ ends into a second band (Figure 4b). As predicted, transcripts with the −66 5′ terminus were undetectable in *ppr53* mutants but accumulated normally in two other non-photosynthetic mutants. The loss of these processed RNAs was not accompanied by an increase in precursors, suggesting that PPR53 functions to stabilize the processed RNAs rather than to promote processing. The poisoned-primer extension data show that approximately 50% of *ndhA* transcripts have the PPR53-dependent 5′ end in wild-type

plants. The two-fold loss of *ndhA* RNA in *ppr53* mutants was not of sufficient magnitude to stand out in the microarray transcriptome data.

Analogous experiments were used to characterize the rRNA deficiencies detected in the transcriptome analysis. RNA gel blot hybridizations confirmed that all plastid rRNAs accumulate to reduced levels in *ppr53* mutants (Figure 5a). The probe for *rrn4.5* and the more downstream of two *rrn23* probes detected a (presumed) precursor of approximately 2 kb that accumulates to increased levels in *ppr53* mutants but not in a different mutant with a plastid rRNA deficiency of similar magnitude (*wtf2*). The Arabidopsis PPR53 ortholog SOT1 is required for the accumulation of a 23S rRNA precursor with a processed 5′ end mapping 73-nucleotides upstream of the mature 23S rRNA (Ian Small, personal communication). A primer extension assay showed that the pre-23S rRNA isoform with this 5′-end is likewise missing in *ppr53* mutants (Figure 5b). This isoform accumulates to normal levels in mutants lacking the closely related protein ATP4, and it is found at elevated levels in the *wtf2* mutant control (see Figure 5a). Interestingly, the PPR53-dependent pre-23S 5′ end was undetectable even in mutants with the mildest visual phenotype (*ppr53-vir*) (Figures 1a and 5b) whereas the severity of the deficiency for mature rRNAs correlated with the severity of the chlorophyll deficiency (Figure 5a). This suggests that the absence of this 23S rRNA precursor is not the sole cause of the loss of plastid ribosomes in *ppr53* mutants.

Recombinant PPR53 binds with specificity to a sequence near the 5′ end of the PPR53-dependent pre-23S rRNA

The “footprints” of some PPR proteins accumulate as small RNAs (sRNAs) *in vivo* due to protection by the bound protein (Ruwe and Schmitz-Linneweber, 2012; Zhelyazkova *et al.*, 2012). An abundant sRNA in wild-type seedlings has a 5′-end matching that of the PPR53-dependent 5′-end upstream from *rrn23* (Figure 5c). This sRNA is missing in *ppr53* mutants (Figure 5c) but accumulates to high levels in *ppr4* mutants, which have a plastid ribosome deficiency of similar magnitude (Schmitz-Linneweber *et al.*, 2006). These results suggested that this sRNA is PPR53’s *in vivo* footprint. Furthermore, the amino acid code for RNA recognition by PPR motifs (Barkan *et al.*, 2012; Yagi *et al.*, 2013a) predicts that the first nine contiguous PPR motifs in PPR53 will bind the sequence UGGAYGUAG (Figure 6a). A very similar sequence, UGGACGUUG, maps near the 5′end of the PPR53-dependent sRNA and pre-23S rRNA (Figure 6b), making this an excellent candidate for a direct PPR53 binding site.

To test whether PPR53 can bind with specificity to this RNA sequence, purified recombinant PPR53 (rPPR53) was used in gel mobility shift assays with various radiolabeled synthetic RNAs (Fig. 6b). PPR53 bound a 24-mer that included its predicted binding site (RNA 23S-A) but did not bind an RNA of similar length from the *petL* 5′UTR that is bound by the PPR protein PGR3 (Cai *et al.*, 2011). This biochemical data, in conjunction with the facts that this RNA includes a strong match to PPR53’s predicted binding site and coincides with a PPR53-dependent sRNA and processed 5′ end, provide strong evidence that PPR53 binds this site *in vivo.* Interestingly, PPR53 failed to bind an RNA that extends 17 nucleotides upstream of the PPR53-dependent 5′ end (RNA 23S-B in Figure 6b). This longer RNA is predicted to fold into a stem-loop structure that includes the

first six nucleotides of the predicted PPR53 binding site in the stem (Figure 6b). Given that sequence-specific interactions between PPR motifs and RNA involve the Watson-Crick face of RNA bases (Yin *et al.*, 2013), it is not surprising that this hairpin impedes protein binding. That being said, the existence of this structure raises the question of how PPR53 gains access to its binding site *in vivo.*

PPR53 also acts at the *ndhA* locus, where it is required both for the accumulation of mRNAs with a processed end 66 nt upstream of the start codon and for optimal translational efficiency. An sRNA with hallmarks of a PPR footprint maps to the PPR53-dependent *ndhA* 5′ end (Ruwe and Schmitz-Linneweber, 2012; Zhelyazkova *et al.*, 2012) and is missing in *ppr53* mutants (Figure S2), suggesting that this may be a direct PPR53 binding site. However, the sequence of this sRNA lacks strong similarity to PPR53's binding site as predicted by the PPR code (Fig. 6a,c). We tested the ability of rPPR53 to bind two synthetic RNAs corresponding to the shorter and longer of the sRNAs mapping to this region (Figure 6c), but neither RNA bound significantly to rPPR53 *in vitro.* These RNAs are not predicted to form stable secondary structures, so RNA-based masking of a binding site is unlikely to account for this negative result. In light of the positive binding results at *rrn23,* these results suggest that PPR53's effects on *ndhA* expression and sRNA accumulation require the participation of another protein.

Discussion

Results presented here show that the PPR-SMR protein PPR53 plays an essential role in the biogenesis of the photosynthetic apparatus by promoting the expression of the chloroplast *ndhA* and *rrn23* genes. PPR53 binds directly to a sequence ~70-nt upstream from the mature 5′ end of 23S rRNA and is required for the accumulation of a pre-23S rRNA isoform with a 5′ end several nucleotides upstream of this binding site. The failure of PPR53 to bind this site is likely to underlie the plastid rRNA deficiencies in *ppr53* mutants, which, in turn, can account for their modest global losses of photosynthetic complexes harboring plastid-encoded proteins. PPR53 is also required for the accumulation of a processed mRNA with a 5′ end mapping 66 nucleotides upstream of *ndhA* and increases *ndhA* translational efficiency. This activity can account for the severe loss of the NDH-like complex in *ppr53* mutants. Genome-wide ribosome profiling and transcriptome assays did not detect any additional chloroplast gene expression defects in *ppr53* mutants, other than minor changes that are likely to be secondary effects. Thus, it seems likely that all aspects of the *ppr53* mutant phenotype arise from the *ndhA* and *rrn23* expression defects.

PPR53's most closely related paralog, ATP4, has also been functionally characterized (Zoschke *et al.*, 2012; Zoschke *et al.*, 2013b). The PPR code predicts that ATP4 and PPR53 bind similar sequences (ATP4-UGGACXUAG; PPR53-UGGAYGUAG- see Figure S1). Nonetheless, the documented functions for these proteins are entirely different. ATP4 is required for the translation of the *atpB* mRNA and interacts *in vivo* with the *atpB* 5′UTR (Zoschke *et al.*, 2012). ATP4 is also required for the accumulation of processed RNAs with termini near *atpF*, *psaJ*, and *rpl14*, but other chloroplast genes are expressed at near normal levels in *atp4* mutants (Zoschke *et al.*, 2012; Zoschke *et al.*, 2013b). It is possible that both PPR53 and ATP4 have additional functions that are redundant and therefore not apparent in

each single mutant. In any case, the distinct mutant phenotypes of *atp4* and *ppr53* mutants highlight the challenges of connecting PPR proteins to their *in vivo* binding sites and functions based solely on current understanding of the amino acid code for RNA recognition by PPR tracts.

Mechanism of PPR53 action at *rrn23*

Our results strongly suggest that PPR53 promotes the biogenesis of the chloroplast 50S ribosomal subunit by binding an RNA sequence spanning approximately −69 to −53 with respect to the 5′ end of mature 23S rRNA. However, it remains unclear how this interaction increases the output of mature ribosomes. PPR53 is a plant-specific protein, but it acts in the context of a ribosome maturation pathway that retains considerable similarity to that in the chloroplast's bacterial ancestor. As in bacteria, chloroplast rRNAs are processed from a single large precursor (reviewed in Deutscher, 2009; Germain *et al.*, 2013). The order of rRNA genes in the chloroplast genome is the same as that in its bacterial ancestor except that the chloroplast 23S and 4.5S rRNAs are derived from the 5′ and 3′ regions, respectively, of the ancestral 23S rRNA (Edwards and Kossel, 1981). In bacteria, rRNA processing is guided by sequences flanking each mature rRNA, which form long-range duplexes that are cleaved by enzymes in the ribonuclease III family (reviewed in Redko *et al.*, 2008; Deutscher, 2009). Additional processing events are carried out by various endo- and exo-ribonucleases, and the final maturation steps are coupled to ribosome assembly and to translational activity itself.

In chloroplasts, a ribonuclease III-family enzyme called Mini-III is believed to cleave a 23S-4.5S rRNA precursor to simultaneously produce the mature 5′ end of 23S rRNA and the 3′ end of 4.5S rRNA (Hotto *et al.*, 2015), in a process that is similar to the final steps in 23S rRNA processing in *B. subtilis* (Redko *et al.*, 2008). The substrate for this cleavage event in chloroplasts is believed to be an RNA duplex of ~20 base pairs formed by complementary sequences in the 5′-proximal region of 23S rRNA and 3′ proximal region of 4.5S rRNA (Takaiwa and Sugiura, 1982; Hotto *et al.*, 2015). As PPR53 binds approximately 30 nucleotides upstream from the sequences involved in this proposed duplex, it is well placed to influence this step in rRNA maturation. This arrangement is reminiscent of that reported for the octotricopeptide repeat protein RAP, which binds upstream of the mature 5′ end of chloroplast 16S rRNA (Kleinknecht *et al.*, 2014) and promotes the accumulation of 30S ribosomal subunits.

How might PPR53 promote the maturation and/or accumulation of 23S rRNA? One consequence of PPR53's binding upstream of *rrn23* is clear: this interaction provides a steric block to a 5′→3′ exonuclease, thereby stabilizing a pre-23S rRNA isoform with a 5′ end at position −69. This view is supported by: (i) the position of the PPR53 binding site immediately downstream of the PPR53-dependent processed 5′ end; (ii) the presence of a PPR53-dependent sRNA spanning the binding site; and (iii) the fact that longer precursors do not accumulate to increased levels in *ppr53* mutants. It is well established that some pure PPR proteins promote the accumulation of processed mRNA isoforms via an analogous barrier mechanism (reviewed in Barkan and Small, 2014). That said, the relationship between PPR53's RNA stabilization effect and its effect on the accumulation of 50S

ribosomal subunits remains uncertain. One possibility is that the pre-23S rRNA isoform that is stabilized by PPR53 is an important intermediate along the rRNA processing pathway. Arguing against this possibility is the fact that this precursor appears to be completely absent in homozygous mutants that exhibit a range of ribosome and pigment deficiencies (see Figures 1 and 5). An alternative possibility is that PPR53 influences the formation of an RNA duplex that guides the concerted 5′ processing of 23S rRNA and 3′ processing of 4.5S rRNA. The 5′ and 3′ portions of this duplex are separated by more than 3000 nucleotides. As such, PPR53 might protect the 5′ proximal region from degradation until the 3′ portion is available for pairing, or it might maintain the 5′ proximal sequences in an unpaired state prior to the availability of its 3′ partner. The RNA stabilization and RNA remodeling scenarios for PPR53 are not mutually exclusive.

How does PPR53 stimulate *ndhA* expression?

PPR53 is required to stabilize transcripts with a 5′-end mapping 66 nucleotides upstream from the *ndhA* start codon, and also increases *ndhA* translational efficiency. Dual RNA stabilization/ translation enhancing effects have been reported for several other helical repeat RNA binding proteins in chloroplasts (Barkan *et al.*, 1994; Vaistij *et al.*, 2000; Felder *et al.*, 2001; Pfalz *et al.*, 2009; Boulouis *et al.*, 2011; Cai *et al.*, 2011; Zoschke *et al.*, 2013b; Lefebvre-Legendre *et al.*, 2015). Several of these proteins have been shown to bind to an RNA segment mapping immediately downstream of the 5′ end they stabilize (Pfalz *et al.*, 2009; Cai *et al.*, 2011; Prikryl *et al.*, 2011; Hammani *et al.*, 2012; Loizeau *et al.*, 2013) and to protect the bound RNA from ribonucleases *in vivo*, as reflected by the accumulation of their “footprints” as sRNAs (Hammani *et al.*, 2012; Ruwe and Schmitz-Linneweber, 2012; Zhelyazkova *et al.*, 2012; Loizeau *et al.*, 2013). The RNA stabilization activity of such proteins results from a steric blockade to 5′→3′ exonucleolytic degradation. An sRNA maps to the 5′ end of PPR53-dependent *ndhA* transcripts (Ruwe and Schmitz-Linneweber, 2012; Zhelyazkova *et al.*, 2012) and fails to accumulate in *ppr53* mutants (Figure S2). The simplest interpretation of these results is that PPR53 binds to the region corresponding to this sRNA and that this interaction simultaneously blocks 5′→3′ degradation and enhances translation. However, there is minimal sequence similarity between the *ndhA* sRNA and the PPR53 binding site as predicted by the PPR code (Figure 6). Furthermore, recombinant PPR53 did not bind this sequence *in vitro* under conditions in which its interaction with the site upstream of *rrn23* was unambiguous. Given this body of data, we favor the possibility that a different, as yet unknown PPR-like protein binds to and protects the 5′proximal region of processed *ndhA* RNA, and that PPR53 promotes this interaction. There is evidence that the PPR-SMR protein ATP4 cooperates with a pure PPR protein in an analogous manner: PPR10 binds the *psaJ* 3′UTR where it blocks 3′→5′ RNA degradation (Pfalz *et al.*, 2009; Prikryl *et al.*, 2011), and ATP4 is required for PPR10’s activity at this site *in vivo* (Zoschke *et al.*, 2012). This cooperation might involve direct protein-protein interactions. Alternatively, the PPR-SMR partner might aid RNA binding by the second protein via transient RNA interactions that reduce occluding secondary structure. In any case, these findings imply that the loss of a particular sRNA in a mutant lacking a PPR-like protein does not always reflect the existence of a direct binding site for that protein within the sRNA sequence.

PPR53 enhances *ndhA* translational efficiency while also stabilizing the −66 processed *ndhA* 5′ end. Several other helical repeat RNA binding proteins acting at distinct chloroplast loci have analogous dual effects on the accumulation of specific processed RNAs and translational efficiency (Barkan *et al.*, 1994; Felder *et al.*, 2001; Pfalz *et al.*, 2009; Cai *et al.*, 2011; Zoschke *et al.*, 2013b; Wang *et al.*, 2015). These correlations can be explained in two ways: either the RNA isoforms that are stabilized by these proteins are intrinsically more translatable than are their precursors, or the presence of the protein a short distance upstream of the start codon stimulates translation. Although we cannot distinguish between these possibilities for PPR53, biochemical evidence supports the latter view for PPR10 and HCF107, whose binding upstream of *atpH* and *psbH*, respectively, precludes the formation of secondary structures that would otherwise occlude the ribosome binding sites (Prikryl *et al.*, 2011; Hammani *et al.*, 2012).

Function of the SMR domain?

A prime motivation for this study was to gain insight into the function of the SMR motif in PPR-SMR proteins. PPR53's stabilization of pre-23S rRNA can be accounted for by a passive barrier effect analogous to that of pure PPR proteins. However, PPR53's effects at *ndhA* and the effects of its paralog ATP4 at *psaJ* cannot be explained by activities attributed thus far to pure PPR proteins. Some SMR domains have endonuclease activity (reviewed in Fukui and Kuramitsu, 2011; Liu *et al.*, 2013) but the molecular defects in *ppr53* mutants do not provide evidence for an endonuclease activity in PPR53. Furthermore, we did not detect endoribonuclease activity when recombinant PPR53 was incubated with radiolabeled RNAs *in vitro* (see unbound RNAs in Figure 6, for example). One possible theme to emerge from the limited body of molecular data for PPR-SMR proteins is suggested by the ability of both ATP4 and PPR53 to support the action of a different protein as an RNA stabilizer (see above). Biochemical analysis of these and other examples will likely be required to elucidate the functions of the enigmatic SMR moiety of proteins in the PPR-SMR subfamily.

Experimental Procedures

Plant material

PPR53 corresponds to maize locus GRMZM2G438524 and is orthologous to Arabidopsis AT5G46580. The *ppr53* mutant alleles were identified during the systematic sequencing of *Mu* transposon insertions in non-photosynthetic mutants in the maize Photosynthetic Mutant Library (Belcher *et al.*, 2015). Molecular analyses used the heteroallelic progeny of complementation crosses between *ppr53-2/+* and *ppr53-3/+* plants. Phenotypically wild-type siblings segregating in the same plantings served as controls. Mutants lacking the closely related protein ATP4 (GRMZM2G128665) (Zoschke *et al.*, 2012; Zoschke *et al.*, 2013b) were included in some assays to illustrate the distinct functions of PPR53 and ATP4. A different ribosome deficient mutant, *wtf2*, was used to control for secondary effects that result from the loss of plastid ribosomes. *csr1* mutants, which lack the thylakoid SRP receptor (Asakura *et al.*, 2004), and *crp1* mutants, which lack a PPR protein required for the expression of several chloroplast ORFs (Zoschke *et al.*, 2013b), were used as additional controls. Plants were grown in soil in cycles of 16 h light (~300 μmol photons × m^{-2} ×

s^{-1})/28 °C and 8 h dark/26°C. Leaf tissue was harvested one hour after the start of the light cycle on the eighth day after sowing, frozen in liquid nitrogen and stored at −80 °C until use.

RNA and protein analyses

RNA was extracted from the second leaf and used for RNA gel blot, primer extension and poisoned primer extension analyses as described (Barkan, 1998; Barkan, 2011b). Probes used for these experiments are shown in Table S1. Proteins were extracted from the apical half of the second leaf. Antibody to Rps12 was purchased from Agrisera (AS12-2114). Antibodies to NdhH and Rpl2 were generously provided by Tsuyoshi Endo (Kyoto University) and Alap Subramanian (University of Arizona), respectively. Other antibodies were generated by us and have been described previously (Zoschke *et al.*, 2012).

Genome wide analyses of the chloroplast transcriptome, translatome, and sRNAs

The ribosome profiling and transcriptome assays were performed as described previously (Zoschke *et al.*, 2013b). The total RNA and ribosome footprint plots shown in Figure 3 are based on two and three biological replicates, respectively. Each biological replicate was analyzed on microarrays with three replicate spots for each probe. Only probes with at least five (of nine) spots (ribosome profiles) or three (of six) spots (total RNA) that passed the background filter (signal>background) are presented in the Figure. Data were normalized as described previously (Zoschke *et al.*, 2013b). The normalized data are available in Dataset S1. The sRNA data were derived from RNAs between ~15 and 40 nucleotides that were purified from seedling leaf RNA. Sequencing libraries were prepared with the NEBNext Multiplex Small RNA Library Prep Set.

In vitro RNA binding assays

The protein coding region of *ppr53* (GRMZM2G438524) minus that encoding the predicted chloroplast targeting sequence was cloned into the pMAL-TEV vector to produce a fusion protein consisting of an N-terminal maltose binding protein, a TEV protease site, and PPR53 starting at amino acid 53. The amino terminus of the protein after TEV cleavage begins "GSPSLSQ...", with the G derived from the vector and the subsequent amino acids from PPR53. Protein was expressed in Arctic Express cells (Agilent). Protein was induced in log phase cultures with 0.5 mM IPTG at 12 °C for 24 h. Purification on amylose beads, TEV cleavage, and gel filtration chromatography on a Superdex 200 column were as described for PPR10 (Pfalz *et al.*, 2009) with the exception that the lysis and column buffer consisted of 40 mM Tris-HCl pH 7.5, 600 mM NaCl and 5 mM β-mercaptoethanol. Lysis buffer additionally contained a protease inhibitor cocktail (Roche complete, EDTA free). Monodisperse protein from the gel filtration column was dialyzed against 25 mM Tris-HCl pH 7.5, 0.5 mM EDTA, 400 mM NaCl, 5 mM β-mercaptoethanol and 50% glycerol and stored at −20°C. Gel mobility shift assays employed synthetic RNAs (IDT) that were radiolabeled at their 5′-end as described previously (Williams-Carrier *et al.*, 2008). The binding reactions contained 50 mM Tris-HCl pH 7.5, 180 mM NaCl, 0.1 mM EDTA, 3 mM DTT, 100 μg/ml Heparin, 20 μg/ml BSA, 10% Glycerol and a maximal protein concentration of 1 μM with 3-fold serial dilutions. Because some SMR domains bind divalent cations, we examined RNA binding and RNA cleavage activities of rPPR53 in the

presence and absence of Mg^{++}, but no differences in activities were detected. Mg^{++} was omitted in the experiments shown here, except in the right panel of Figure 6c in which rPPR53 was preincubated on ice with 15 mM $MgCl_2$ and used in the RNA binding reactions at a final concentration of 3 mM $MgCl_2$.

Supplementary Material

Refer to Web version on PubMed Central for supplementary material.

Acknowledgments

We are grateful to Tiffany Kroeger for technical assistance, Roz Williams-Carrier for identifying insertions in *ppr53*, Susan Belcher for mutant propagation, Margarita Rojas for preparing figures, and Ian Small and Kate Howell (University of Western Australia) for helpful discussions and sharing of data. This work was supported by grants from the National Science Foundation to A.B. (MCB-1243641 and IOS-1339130), by a postdoctoral fellowship from the Deutsche Forschungsgemeinschaft to R.Z. (Grants Zo 302/1-1 and Zo 302/2-1), and by NIH training grant 7T32GM007759 (R.G.M.).

References

Asakura Y, Hirohashi T, Kikuchi S, Belcher S, Osborne E, Yano S, Terashima I, Barkan A, Nakai M. Maize mutants lacking chloroplast FtsY exhibit pleiotropic defects in the biogenesis of thylakoid membranes. Plant Cell. 2004; 16:201–214. [PubMed: 14688289]

Barkan A. Approaches to investigating nuclear genes that function in chloroplast biogenesis in land plants. Methods Enzymol. 1998; 297:38–57.

Barkan A. Expression of plastid genes: organelle-specific elaborations on a prokaryotic scaffold. Plant Physiol. 2011a; 155:1520–1532. [PubMed: 21346173]

Barkan, A. Studying the structure and processing of chloroplast transcripts. In: Jarvis, P., editor. Chloroplast research in Arabidopsis: Methods and protocols. New York: Humana Press; 2011b. p. 183-197.

Barkan A, Rojas M, Fujii S, Yap A, Chong YS, Bond CS, Small I. A combinatorial amino acid code for RNA recognition by pentatricopeptide repeat proteins. PLoS Genetics. 2012; 8:e1002910. [PubMed: 22916040]

Barkan A, Small I. Pentatricopeptide Repeat Proteins in Plants. Annu Rev Plant Biol. 2014; 65:415–442. [PubMed: 24471833]

Barkan A, Walker M, Nolasco M, Johnson D. A nuclear mutation in maize blocks the processing and translation of several chloroplast mRNAs and provides evidence for the differential translation of alternative mRNA forms. EMBO J. 1994; 13:3170–3181. [PubMed: 8039510]

Belcher S, Williams-Carrier R, Stiffler N, Barkan A. Large-scale genetic analysis of chloroplast biogenesis in maize. Biochim Biophys Acta. 2015; 1847:1004–1016. [PubMed: 25725436]

Boulouis A, Raynaud C, Bujaldon S, Aznar A, Wollman FA, Choquet Y. The nucleus-encoded trans-acting factor MCA1 plays a critical role in the regulation of cytochrome f synthesis in Chlamydomonas chloroplasts. Plant Cell. 2011; 23:333–349. [PubMed: 21216944]

Cai W, Okuda K, Peng L, Shikanai T. PROTON GRADIENT REGULATION 3 recognizes multiple targets with limited similarity and mediates translation and RNA stabilization in plastids. Plant J. 2011; 67:318–327. [PubMed: 21457370]

del Campo EM, Sabater B, Martin M. Transcripts of the ndhH-D operon of barley plastids: possible role of unedited site III in splicing of the ndhA intron. Nucleic Acids Res. 2000; 28:1092–1098. [PubMed: 10666448]

Deutscher MP. Maturation and degradation of ribosomal RNA in bacteria. Prog Molecular Biology and Translational Sci. 2009; 85:369–391.

Edwards K, Kossel H. The rRNA operon from Zea mays chloroplasts: nucleotide sequence of 23S rDNA and its homology with E.coli 23S rDNA. Nucleic Acids Res. 1981; 9:2853–2869. [PubMed: 7024906]

Felder S, Meurer J, Meierhoff K, Klaff P, Bechtold N, Westhoff P. The nucleus-encoded HCF107 gene of Arabidopsis provides a link between intercistronic RNA processing and the accumulation of translation-competent psbH transcripts in chloroplasts. Plant Cell. 2001; 13:2127–2141. [PubMed: 11549768]

Fujii S, Sato N, Shikanai T. Mutagenesis of individual pentatricopeptide repeat motifs affects RNA binding activity and reveals functional partitioning of Arabidopsis PROTON gradient regulation3. Plant Cell. 2013; 25:3079–3088. [PubMed: 23975900]

Fukui K, Kuramitsu S. Structure and Function of the Small MutS-Related Domain. Molecular Biology International. 2011; 2011:691735. [PubMed: 22091410]

Germain A, Hotto AM, Barkan A, Stern DB. RNA processing and decay in plastids. Wiley Interdisciplinary Reviews RNA. 2013; 4:295–316. [PubMed: 23536311]

Haili N, Arnal N, Quadrado M, Amiar S, Tcherkez G, Dahan J, Briozzo P, Colas des Francs-Small C, Vrielynck N, Mireau H. The pentatricopeptide repeat MTSF1 protein stabilizes the nad4 mRNA in Arabidopsis mitochondria. Nucleic Acids Res. 2013; 41:6650–6663. [PubMed: 23658225]

Hammani K, Bonnard G, Bouchoucha A, Gobert A, Pinker F, Salinas T, Giege P. Helical repeats modular proteins are major players for organelle gene expression. Biochimie. 2014; 100C:141–150. [PubMed: 24021622]

Hammani K, Cook W, Barkan A. RNA binding and RNA remodeling activities of the Half-a-Tetratricopeptide (HAT) protein HCF107 underlie its effects on gene expression. PNAS. 2012; 109:5651–5656. [PubMed: 22451905]

Hammani K, Giege P. RNA metabolism in plant mitochondria. Trends in Plant Sci. 2014; 19:380–389. [PubMed: 24462302]

Hotto AM, Castandet B, Gilet L, Higdon A, Condon C, Stern DB. Arabidopsis Chloroplast Mini-Ribonuclease III Participates in rRNA Maturation and Intron Recycling. Plant Cell. 2015; 27:724–740. [PubMed: 25724636]

Ifuku K, Endo T, Shikanai T, Aro EM. Structure of the chloroplast NADH dehydrogenase-like complex: nomenclature for nuclear-encoded subunits. Plant & Cell Physiol. 2011; 52:1560–1568. [PubMed: 21785130]

Kleinknecht L, Wang F, Stube R, Philippar K, Nickelsen J, Bohne AV. RAP, the sole octotricopeptide repeat protein in Arabidopsis, is required for chloroplast 16S rRNA maturation. Plant Cell. 2014; 26:777–787. [PubMed: 24585838]

Koussevitzky S, Nott A, Mockler TC, Hong F, Sachetto-Martins G, Surpin M, Lim J, Mittler R, Chory J. Signals from chloroplasts converge to regulate nuclear gene expression. Science. 2007; 316:715–719. [PubMed: 17395793]

Lefebvre-Legendre L, Choquet Y, Kuras R, Loubery S, Douchi D, Goldschmidt-Clermont M. A nucleus-encoded chloroplast protein regulated by iron availability governs expression of the photosystem I subunit PsaA in Chlamydomonas reinhardtii. Plant Physiol. 2015; 167:1527–1540. [PubMed: 25673777]

Liu S, Melonek J, Boykin LM, Small I, Howell KA. PPR-SMRs: Ancient proteins with enigmatic functions. RNA Biol. 2013; 10:1501–1510. [PubMed: 24004908]

Liu X, Yu F, Rodermel S. An Arabidopsis pentatricopeptide repeat protein, SUPPRESSOR OF VARIEGATION7, is required for FtsH-mediated chloroplast biogenesis. Plant Physiol. 2010; 154:1588–1601. [PubMed: 20935174]

Loizeau K, Qu Y, Depp S, Fiechter V, Ruwe H, Lefebvre-Legendre L, Schmitz-Linneweber C, Goldschmidt-Clermont M. Small RNAs reveal two target sites of the RNA-maturation factor Mbb1 in the chloroplast of Chlamydomonas. Nucleic Acids Res. 2014; 42:3286–3297. [PubMed: 24335082]

Lurin C, et al. Genome-wide analysis of Arabidopsis pentatricopeptide repeat proteins reveals their essential role in organelle biogenesis. Plant Cell. 2004; 16:2089–2103. [PubMed: 15269332]

Majeran W, Friso G, Asakura Y, Qu X, Huang M, Ponnala L, Watkins KP, Barkan A, van Wijk KJ. Nucleoid-enriched proteomes in developing plastids and chloroplasts from maize leaves: a new conceptual framework for nucleoid functions. Plant Physiol. 2012; 158:156–189. [PubMed: 22065420]

Pfalz J, Bayraktar O, Prikryl J, Barkan A. Site-specific binding of a PPR protein defines and stabilizes 5′ and 3′ mRNA termini in chloroplasts. EMBO J. 2009; 28:2042–2052. [PubMed: 19424177]

Pfalz J, Liere K, Kandlbinder A, Dietz KJ, Oelmuller R. pTAC2, -6, and -12 are components of the transcriptionally active plastid chromosome that are required for plastid gene expression. Plant Cell. 2006; 18:176–197. [PubMed: 16326926]

Prikryl J, Rojas M, Schuster G, Barkan A. Mechanism of RNA stabilization and translational activation by a pentatricopeptide repeat protein. Proc Natl Acad Sci USA. 2011; 108:415–420. [PubMed: 21173259]

Redko Y, Bechhofer DH, Condon C. Mini-III, an unusual member of the RNase III family of enzymes, catalyses 23S ribosomal RNA maturation in B. subtilis. Molecular Microbiology. 2008; 68:1096–1106. [PubMed: 18363798]

Ruwe H, Schmitz-Linneweber C. Short non-coding RNA fragments accumulating in chloroplasts: footprints of RNA binding proteins? Nucleic Acids Res. 2012; 40:3106–3116. [PubMed: 22139936]

Schmitz-Linneweber C, Williams-Carrier RE, Williams-Voelker PM, Kroeger TS, Vichas A, Barkan A. A Pentatricopeptide Repeat Protein Facilitates the trans-Splicing of the Maize Chloroplast *rps12* Pre-mRNA. Plant Cell. 2006; 18:2650–2663. [PubMed: 17041147]

Small I, Peeters N. The PPR motif - a TPR-related motif prevalent in plant organellar proteins. Trends Biochem Sci. 2000; 25:46–47. [PubMed: 10664580]

Takaiwa F, Sugiura M. The complete nucleotide sequence of a 23-S rRNA gene from tobacco chloroplasts. Eur J Biochem. 1982; 124:13–19. [PubMed: 6177532]

Takenaka M, Zehrmann A, Brennicke A, Graichen K. Improved computational target site prediction for pentatricopeptide repeat RNA editing factors. PloS One. 2013; 8:e65343. [PubMed: 23762347]

Vaistij FE, Boudreau E, Lemaire SD, Goldschmidt-Clermont M, Rochaix JD. Characterization of Mbb1, a nucleus-encoded tetratricopeptide-like repeat protein required for expression of the chloroplast psbB/psbT/psbH gene cluster in Chlamydomonas reinhardtii. Proc Natl Acad Sci U S A. 2000; 97:14813–14818. [PubMed: 11121080]

Wang F, Johnson X, Cavaiuolo M, Bohne AV, Nickelsen J, Vallon O. Two Chlamydomonas OPR proteins stabilize chloroplast mRNAs encoding small subunits of photosystem II and cytochrome b_6f. Plant J. 2015; 82:861–873. [PubMed: 25898982]

Williams-Carrier R, Kroeger T, Barkan A. Sequence-specific binding of a chloroplast pentatricopeptide repeat protein to its native group II intron ligand. RNA. 2008; 14:1930–1941. [PubMed: 18669444]

Williams-Carrier R, Zoschke R, Belcher S, Pfalz J, Barkan A. A major role for the plastid-encoded RNA polymerase complex in the expression of plastid transfer RNAs. Plant Physiol. 2014; 164:239–248. [PubMed: 24246379]

Yagi Y, Hayashi S, Kobayashi K, Hirayama T, Nakamura T. Elucidation of the RNA recognition code for pentatricopeptide repeat proteins involved in organelle RNA editing in plants. PloS One. 2013a; 8:e57286. [PubMed: 23472078]

Yagi Y, Tachikawa M, Noguchi H, Satoh S, Obokata J, Nakamura T. Pentatricopeptide repeat proteins involved in plant organellar RNA editing. RNA Biol. 2013b; 10:1419–1425. [PubMed: 23669716]

Yin P, et al. Structural basis for the modular recognition of single-stranded RNA by PPR proteins. Nature. 2013; 504:168–171. [PubMed: 24162847]

Zhelyazkova P, Hammani K, Rojas M, Voelker R, Vargas-Suarez M, Borner T, Barkan A. Protein-mediated protection as the predominant mechanism for defining processed mRNA termini in land plant chloroplasts. Nucleic Acids Res. 2012; 40:3092–3105. [PubMed: 22156165]

Zoschke R, Kroeger T, Belcher S, Schottler MA, Barkan A, Schmitz-Linneweber C. The Pentatricopeptide Repeat-SMR Protein ATP4 promotes translation of the chloroplast atpB/E mRNA. Plant J. 2012; 72:547–558. [PubMed: 22708543]

Zoschke R, Qu Y, Zubo YO, Borner T, Schmitz-Linneweber C. Mutation of the pentatricopeptide repeat-SMR protein SVR7 impairs accumulation and translation of chloroplast ATP synthase subunits in Arabidopsis thaliana. J Plant Res. 2013a; 126:403–414. [PubMed: 23076438]

Zoschke R, Watkins K, Barkan A. A rapid microarray-based ribosome profiling method elucidates chloroplast ribosome behavior *in vivo*. Plant Cell. 2013b; 25:2265–2275. [PubMed: 23735295]

Author Manuscript

Author Manuscript

Author Manuscript

Significance Statement

PPR-SMR proteins are nucleic acid-binding proteins found in plant chloroplasts and mitochondria. Members of this protein family have diverse effects on plant physiology, but little is known about their direct molecular activities. Here we show that one PPR-SMR protein is a sequence-specific RNA binding protein that promotes the expression of two chloroplast genes by influencing the stability, processing, and translation of their RNAs.

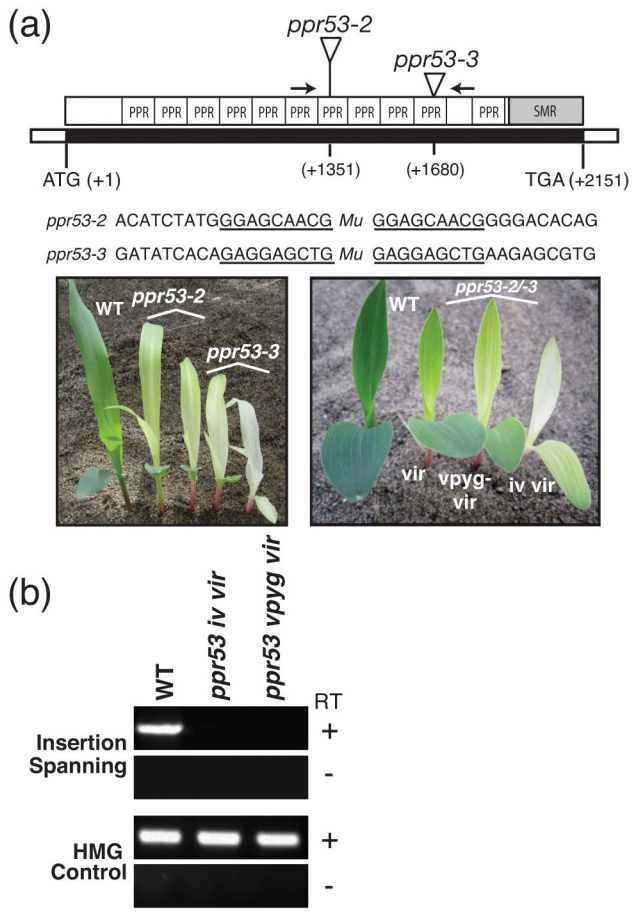

Figure 1. Overview of *ppr53* mutant alleles

(a) The *ppr53* gene (locus GRMZM2G438524) lacks introns. Positions of the *Mu* insertions in alleles characterized here are diagrammed in the context of the domain architecture of the PPR53 protein. The sequence context of each insertion including the 9 bp target site duplication (underlined) and the phenotypes of the plants are shown below. Plants were grown for 8 days in soil. Plants that are homozygous for each single allele (left) as well as the heteroallelic progeny of complementation crosses (right) exhibit variable chlorotic phenotypes (vir-virescent; vpyg-very pale yellow green; iv-ivory). Arrows mark the positions of primers used for RT-PCR in panel (*b).*

(b) Reverse-transcriptase PCR demonstrating the absence of *ppr53* mRNA in *ppr53* mutants. Seedling leaf RNA from *ppr53-2/ppr53-3* mutant individuals with the indicated pigment phenotypes (see panel *a*) was analyzed by RT-PCR, using primers that flank the insertions (see arrows in panel (a)). Reactions lacking reverse transcriptase (RT) and amplification of mRNA encoding High Mobility Group (HMG) protein (GRMZM2G024976) were performed as negative and positive controls, respectively.

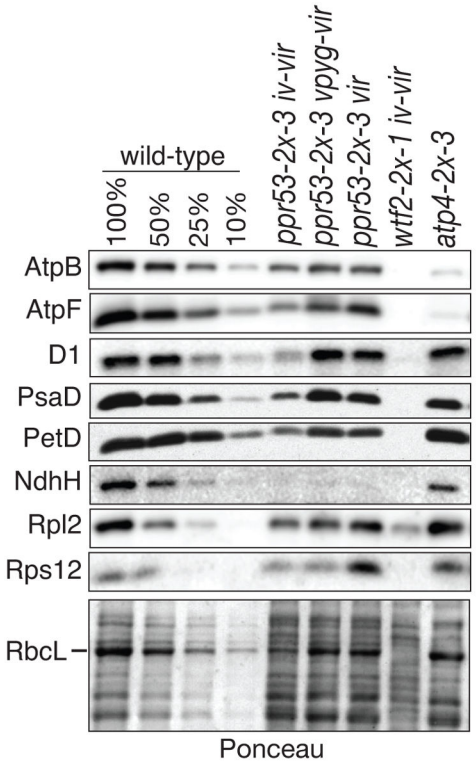

Figure 2. Immunoblot analysis of core subunits of photosynthetic complexes in *ppr53* mutants

Replicate immunoblots of seedling leaf extract (5 μg protein or the indicated dilutions) were probed with antibodies specific for subunits of the ATP synthase (AtpB, AtpF), photosystem II (D1), photosystem I (PsaD), the cytochrome b_6f complex (PetD), the NADH dehydrogenase (NdhH), and the large and small ribosomal subunits (Rpl2 and Rps12, respectively). RbcL (the large subunit of Rubisco) can be seen on the Ponceau S-stained blot below. A mutant lacking the PPR53 paralog ATP4 (Zoschke *et al.*, 2012) and a mutant with a plastid ribosome deficiency similar in magnitude to *ppr53* mutants (*wtf2*, whose ribosome deficiency is documented below) were included for comparison. Mutant samples are annotated with their pigment phenotypes as defined in Figure 1a.

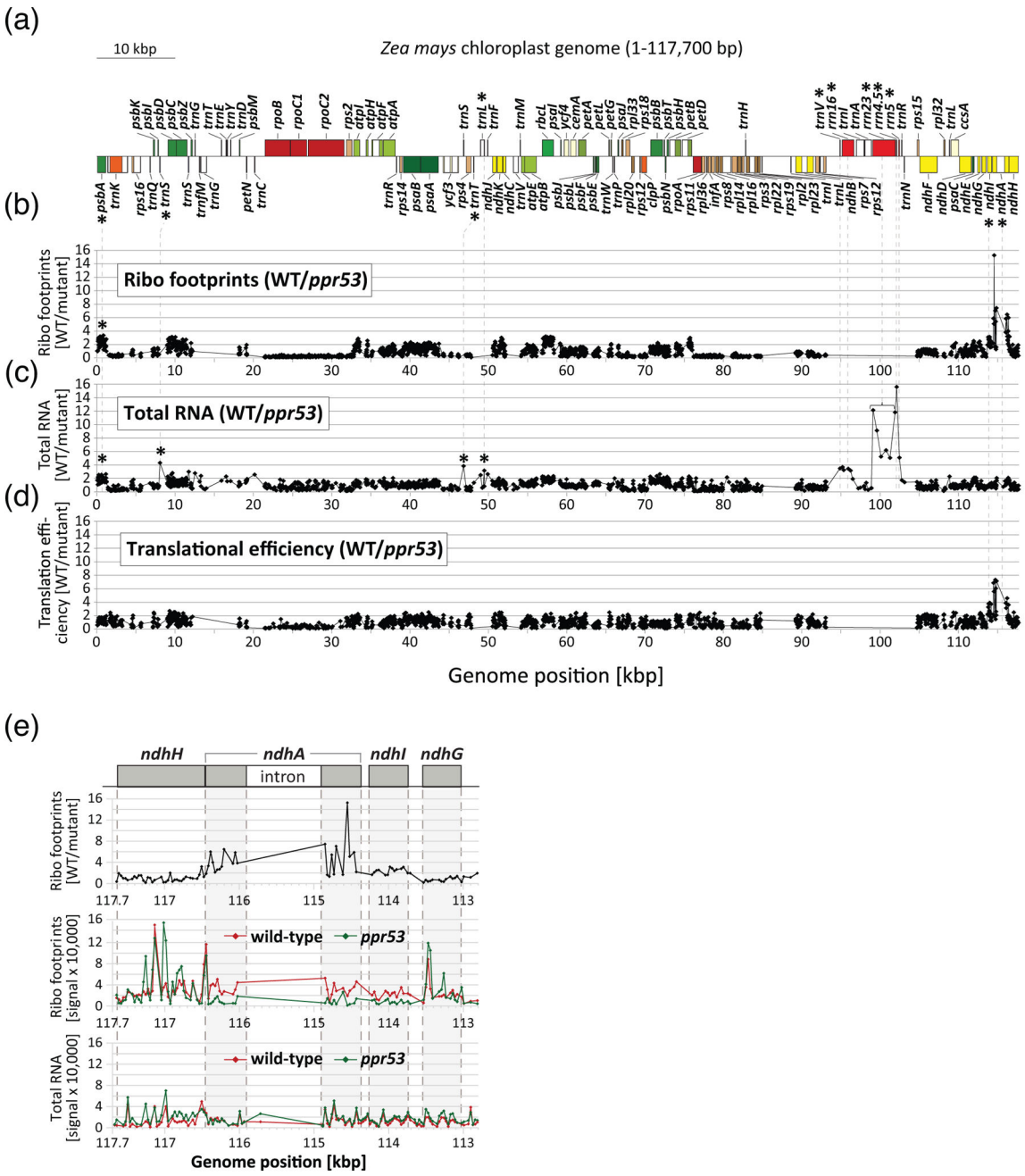

Figure 3. Genome-wide analyses of the chloroplast translatome and transcriptome in *ppr53* mutants. The data used to generate these plots are provided in Data S1

(a) Map of the maize chloroplast genome showing just one of the two large inverted repeats. Asterisks mark genes showing reduced expression in *ppr53* mutants.

(b) Ratio of ribosome footprint signals in the wild-type relative to *ppr53* mutants. Heteroallelic progeny of complementation crosses with a mild pigment phenotype (*vir* seedlings in Figure 1a) were used for these experiments.

(c) Ratio of RNA abundance in the wild-type relative to *ppr53* mutants. RNA extracted from an aliquot of the material used for ribosome profiling was hybridized to a replicate microarray.

(d) Relative translational efficiencies were calculated as the ratio of ribosome footprint ratios to the total RNA ratios.

(e) High resolution view of data from the *ndhA* region. The upper panel shows the ratio of ribosome footprint signal in wild-type relative to the mutant, whereas the lower panels show the individual wild-type and mutant values for both ribosome footprints and total RNA. Two regions in *ndhH* show much stronger ribosome footprint signal in the mutant than in the wild-type (see middle panel); this was a reproducible finding but its basis is unknown. Data points from the *ndhA* intron are sparse (RNA) or absent (ribosome footprints) due to sparse coverage on the array and low signal.

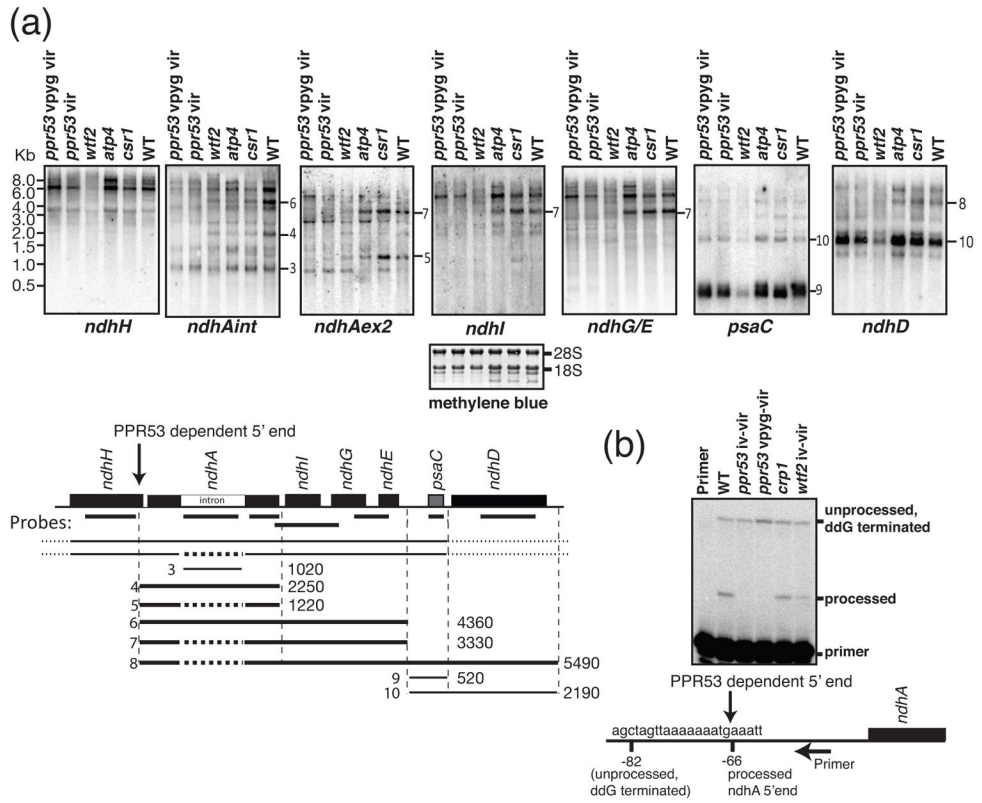

Figure 4. Analysis of *ndhA* transcripts in *ppr53* mutants

(a) RNA gel blot analysis of transcripts from the *ndhA* transcription unit. Replicate blots of seedling leaf RNA (5 μg) were hybridized to the probes indicated on the map below. Two heteroallelic *ppr53* individuals with distinct pigment phenotypes (vpyg vir and vir; see Figure 1) were analyzed. RNA from *atp4*, *wtf2*, and *csr1* mutants was analyzed for comparison; *wtf2* mutants have a plastid rRNA deficiency that is similar in magnitude to that of *ppr53* mutants (see Figure 5), whereas *csr1* mutants have pleiotropic losses of thylakoid membrane complexes due to the absence of the chloroplast SRP receptor (Asakura *et al.*, 2004). A representative methylene blue stained blot is shown below as a loading control. Transcripts whose positions could be confidently assigned based on these results are diagrammed below the map, annotated with their approximate length in nucleotides; thick lines denote transcripts that are missing in *ppr53* mutants. Spliced transcripts are illustrated with a dashed line in the place of the *ndhA* intron.

(b) Poisoned-primer extension assay to display the ratio of processed to unprocessed transcripts with a 5′ end 66 nucleotides upstream of *ndhA.* A primer mapping a short distance downstream of the processed 5′ end was used in a reverse transcription reaction with seedling leaf RNA. Dideoxyguanosine (ddG) was included to terminate reverse transcription on unprocessed RNA at the first cytidine residue upstream of the processed end.

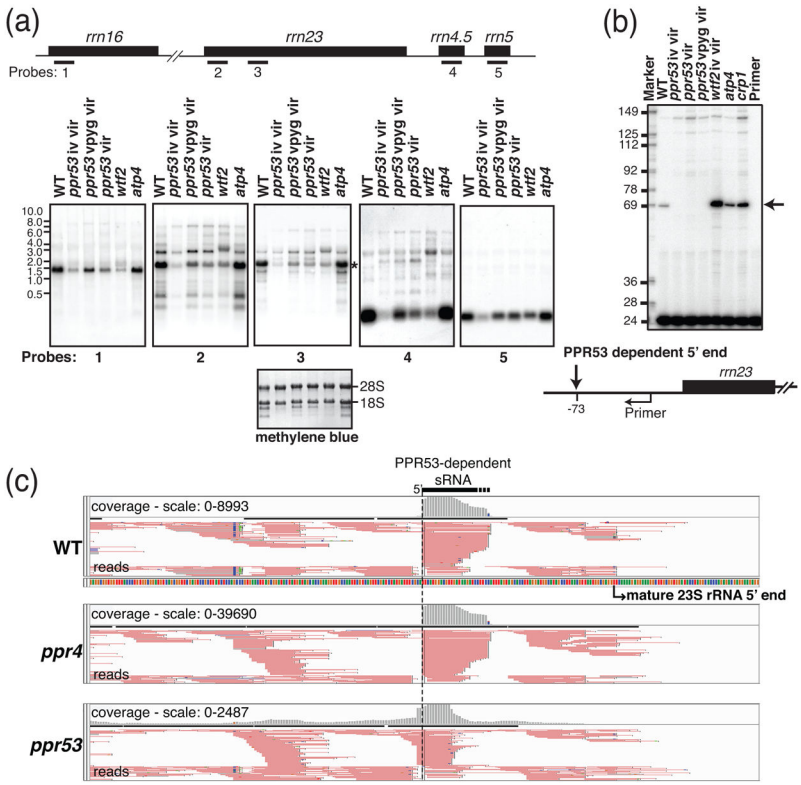

Figure 5. Analysis of chloroplast rRNAs in *ppr53* mutants

(a) RNA gel blot analysis of transcripts from the *rrn* transcription unit. Replicate blots of seedling leaf RNA were hybridized to the probes indicated on the map. Three heteroallelic *ppr53* individuals with distinct pigment phenotypes (iv vir, vpyg vir and vir; see Figure 1) were analyzed. RNAs from the non-photosynthetic mutants *atp4* and *wtf2* were analyzed for comparison. The *wtf2* mutant is shown to illustrate pleiotropic effects resulting from the loss of plastid ribosomes. An image of one of the blots stained with methylene blue is shown below to illustrate equal loading of cytosolic 28S and 18S rRNAs.

(b) Primer extension assay to quantify processed transcripts with a 5′-end mapping 70 nucleotides upstream of *rrn23.* A 5′-end labeled 24-nucleotide primer starting four nucleotides upstream of mature 23S rRNA was used to prime reverse transcription on 5 μg seedling leaf RNA. The ribosome-deficient mutant *wtf2* (see panel a) as well as two other non-photosynthetic mutants (*atp4* and *crp1)* accumulate increased levels of the −70 23S rRNA precursor (see arrow), whereas it is undetectable in all three *ppr53* mutant individuals. The abundance of longer *rrn23* processing intermediates is similar in all mutant samples analyzed, as shown also on the RNA gel blot in panel *a* (see probe 2 data).

(c) PPR53-dependent sRNA mapping to the 5′ end of the PPR53-dependent *rrn23* precursor. Screen captures from the Integrated Genome Viewer show reads as pink lines and a histogram of read counts in gray (above). The 5′-end of the PPR53-dependent sRNAs corresponds with that of the PPR53-dependent pre-23S rRNA. sRNA reads from flanking regions serve as internal standards. Data from a *ppr4* mutant are shown to control for effects resulting from the loss of plastid ribosomes. The loss of this PPR53-dependent sRNA is

accompanied by an increase in the abundance of an sRNA with a 5′-end 2-nucleotides upstream. The basis for this effect is unknown.

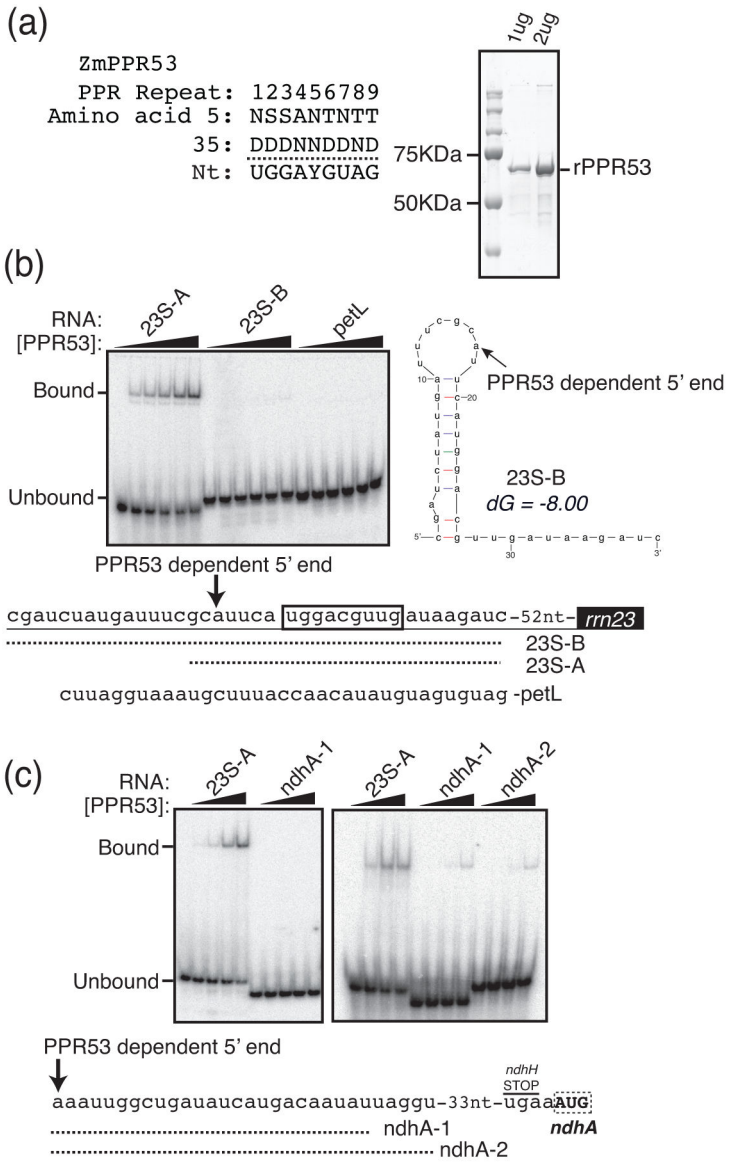

Figure 6. RNA binding activities of recombinant PPR53

(a) Predicted PPR53 sequence specificity. The identities of the fifth and 35th amino acid in each of the first nine PPR motifs in PPR53 are shown (amino acid numbering scheme of (Yin *et al.*, 2013)), along with the predicted nucleotide specificity of each repeat (Barkan *et al.*, 2012). The 10th PPR motif was not included in the prediction because its highly degenerate sequence does not suggest a nucleotide preference based on current understanding of the PPR code. The final PPR motif, which sits adjacent to the SMR domain, was not considered because it is not contiguous with the first ten motifs. A Coomassie-stained SDS-polyacrylamide gel of recombinant PPR53 (rPPR53) is shown to the right.

(b) Gel mobility shift assay showing interaction between rPPR53 and an RNA mapping to the 5′ proximal region of the PPR53-dependent pre-23S rRNA isoform. The sequences of the three radiolabeled RNAs are shown below. The predicted binding site of PPR53 is boxed

and the position of the PPR53-dependent 5′ end is marked with an arrow. Reactions contained 100 pmol RNA and protein at 0 nM, 12 nM, 37 nM, 110 nM, 330 nM, or 1 μM. The predicted secondary structure (Mfold, with default parameters) of the 23S-B RNA is shown to the right. (c) Gel mobility shift assays to detect an interaction between PPR53 and the *ndhA* 5′UTR. Reactions contained 100 pmol RNA and protein as in (b) except that the 12 nM dilution was omitted. The sequences of the two *ndhA* RNAs are shown below. These RNAs correspond to short and long versions of an sRNA detected in barley (Zhelyazkova *et al.*, 2012) and maize (Figure S2). All binding assays were performed under identical conditions with one exception: binding assays shown in the right panel of Figure 6c included 3 mM $MgCl_2$ whereas the other assays lacked $MgCl_2$.